

# The Ongoing Seismic Sequence at the Pollino Mountains, Italy

by Cristina Totaro, Debora Presti, Andrea Billi, Anna Gervasi, Barbara Orecchio, Ignazio Guerra, and Giancarlo Neri

## INTRODUCTION

A sequence of thousands of small to moderate earthquakes has been occurring since spring 2010 in the Pollino Mountains area, southern Italy (Fig. 1), where a seismic gap was previously hypothesized by paleoseismological evidence associated with the lack of major earthquakes in historical catalogs (Michetti *et al.*, 2000; Cinti *et al.*, 2002). Seismic activity is in progress at the time of writing of this paper (December 2012) after quite a disturbing long-term acceleration of earthquake rate and strain release (Fig. 1b). The strongest earthquake ( $M_L$  5.0 according to the Italian Seismological Instrumental and parametric Database [ISIDE], <http://iside.rm.ingv.it>; last accessed September 2013) was recorded on 25 October 2012 and produced damage in the epicentral area corresponding to a maximum intensity of 6 on the European Macroseismic Scale 1998 (EMS-98) in the localities of Mormanno, Campotenese, and Piano Incoronata (Fig. 2; D'Amico and Scarfi, 2012). Because of this earthquake, more than a thousand people were evacuated from their homes and emergency actions have been carried out by the competent institutions. This earthquake with its effects, and the increasing number and intensity of events felt by the population in the preceding months, have further encouraged the attention and efforts of civil defense operators and scientific researchers toward this peculiar seismic crisis occurring in a presumed seismic-gap area. It should also be remarked that the Pollino area, lying at the northern edge of the Calabrian subduction zone (Fig. 1a), represents a highly deformed, very intricate sector of great geodynamic interest and still not fully understood (see, e.g., Bonini *et al.*, 2011; Frepoli *et al.*, 2011; Spina *et al.*, 2011; Neri *et al.*, 2012). The present study, which focuses on the ongoing Pollino sequence in the framework of the seismotectonic processes occurring in the wider area of northern Calabria and the southern Apennines, draws benefit from enhancement of seismic monitoring carried out by national and local research institutions during the ongoing seismic crisis (Fig. 3).

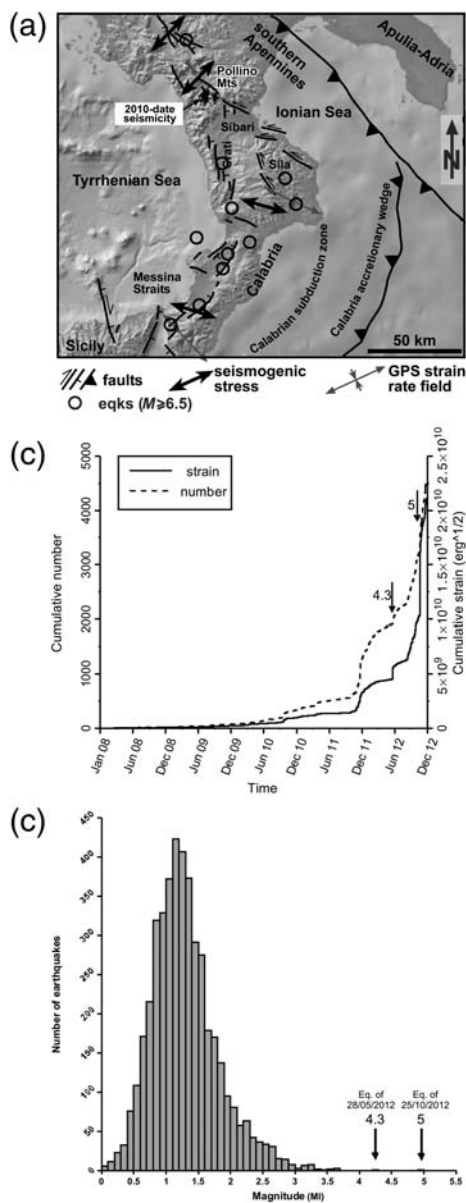
## GEOLOGICAL SETTING

The Pollino Mountains are located in the northern section of the Calabrian accretionary wedge, which, since at least the Neogene, has been drifting southeastward onto the retreating Ionian subducting slab (Fig. 1a; Billi *et al.*, 2006, 2007; Neri *et al.*, 2012). During the rollback process, the northwestward-

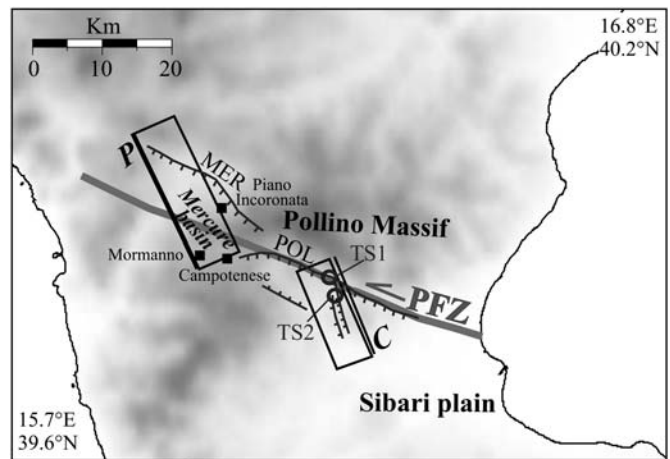
subducting slab has undergone a progressive reduction in its along-strike length up to the present size (Faccenna *et al.*, 2011), which is about 150 km between the Straits of Messina and the Sila Massif (Fig. 1a; see also Neri *et al.*, 2009; Billi *et al.*, 2010). At the northern edge of the Calabrian subduction zone (Fig. 1a), the Pollino Mountains lie in a junction area between the subduction zone itself and the southern Apennines extensional domain. Previous studies have indicated this as a highly deformed zone including shallow dynamics associated with the activity of a Subduction–Transform Edge Propagator (STEP) fault (Neri *et al.*, 2012; Presti *et al.*, 2013).

Calabria and the southern Apennines are among the most seismically active regions of the entire Mediterranean area with their long record of destructive historical earthquakes of magnitude as large as 7 (Monaco and Tortorici, 2000; Galli and Bosi, 2003; Amoroso *et al.*, 2006; Neri *et al.*, 2006; Guidoboni *et al.*, 2007; Galli *et al.*, 2008; the locations of the  $M$  6.5+ earthquakes reported in the CPTI11 catalog are indicated by circles in Fig. 1a). In Calabria, the strongest earthquakes can be ascribed to an extensional regime with opening direction varying from east–west in central Calabria to northwest–southeast in southern Calabria and the Straits of Messina (see e.g., Neri *et al.*, 2004, 2005). In the southern Apennines, major earthquakes are related to northeast–southwest extension (Billi *et al.*, 2011; Presti *et al.*, 2013). Between Calabria and the southern Apennines, the Pollino area has been affected only by moderate seismicity in the last centuries, as witnessed by historical and recent catalogs reporting earthquakes of maximum magnitude in the range 5.5–6, such as those, which occurred in 1693, 1708, and 1998 (see e.g., Galli *et al.*, 2001; Arrigo *et al.*, 2006; Rovida *et al.*, 2011). On the other hand, paleoseismological investigations have identified in the southern Pollino area at least two surface-faulting events between the sixth and fifteenth centuries A.D. relating to earthquakes of magnitude 6.5–7 (Michetti *et al.*, 2000; Cinti *et al.*, 2002; trench site locations are indicated in Fig. 2). This information has led the same investigators to propose the Pollino area as a seismic gap.

The structural and seismotectonic setting of the Pollino area is quite intricate and different views have been proposed by different authors (see, among others, Michetti *et al.*, 2000; Catalano *et al.*, 2004; Database of Individual Seismogenic Sources [DISS] Working Group, 2010; Spina *et al.*, 2011). Although normal mechanisms on northwest-trending structures represent the most diffuse faulting style, diversely oriented structures



▲ **Figure 1.** (a) Tectonic setting of the southern Apennines and Calabria region, southern Italy. Dots, earthquake locations of the ongoing seismic crisis in the Pollino Mountains (2010 to date seismicity; see also Fig. 4a); circles, locations of the earthquakes of magnitude 6.5 and larger that occurred after 1000 A.D. according to the CPT11 catalog (Rovida *et al.*, 2011; <http://emidius.mi.ingv.it/CPT11/>, last accessed September 2013). Seismogenic stresses are from Montone *et al.* (2012), and Global Positioning System (GPS) strain-rate fields are from Billi *et al.* (2011). (b) Cumulative number and strain release of earthquakes of the Pollino area from January 2008 to December 2012. Arrows show the timing of the two strongest earthquakes of the ongoing activity: the magnitude 5.0 earthquake of 25 October 2012, and the magnitude 4.3 earthquake of 28 May 2012, respectively. (c) Frequency–magnitude earthquake distribution reported in the Italian Seismological Instrumental and parametric Data-basE (ISIDE) (<http://iside.rm.ingv.it>, last accessed September 2013) for the Pollino area between 1 April 2010 and 5 December 2012. Arrows indicate the two strongest earthquakes of the ongoing activity.



▲ **Figure 2.** In this map of the Pollino Mountains area, rectangles represent the surface projections of the two sources reported in the Database of Individual Seismic Sources (DISS Working Group, 2010; <http://diss.rm.ingv.it/diss/>, last accessed September 2013): *P* is a normal-faulting east-dipping north-northwest-trending source located in the Mercure basin area, whereas *C* is a normal-faulting west-dipping north-northwest-trending source located in the southern side of the Pollino Massif. We also show the traces of the main active faults reported by Michetti *et al.* (2000) and the Pollino fault zone (PFZ) proposed by Van Dijk *et al.* (2000) and more recently by other investigators (e.g., Spina *et al.*, 2011). Following Michetti *et al.* (2000), MER and POL stand for Mercure and Pollino fault, respectively. Small squares indicate the three localities where the maximum macroseismic intensity was recorded for the magnitude 5.0 earthquake of 25 October 2012 (D’Amico and Scarfi, 2012). Circles show the trench sites (TS1 and TS2) where paleoseismological investigations identified faulting events relatable to earthquakes of magnitude 6.5–7, which occurred between the sixth and fifteenth centuries A.D. (Michetti *et al.*, 2000; Cinti *et al.*, 2002).

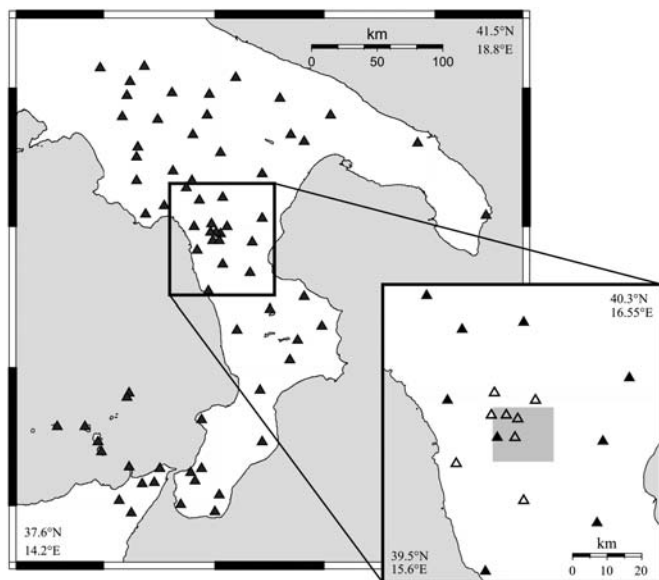
and different mechanisms are also reported, such as left-lateral strike-slip kinematics in the west-northwest-trending Pollino fault zone (PFZ) on the southern side of the Massif (Van Dijk *et al.*, 2000; Catalano *et al.*, 2004; Spina *et al.*, 2011; see Fig. 2). The Database of Individual Seismogenic Sources (DISS Working Group, 2010) reports two normal-faulting sources in the Pollino area, an east-dipping north-northwest-trending one in the Mercure basin area (*P* in Fig. 2) and a west-dipping north-northwest-trending one in the southern side of the Massif (*C* in Fig. 2). In contrast, at the same location of the *P* source, Michetti *et al.* (2000) report a west-northwest-striking south-west-dipping normal fault (MER, Fig. 2), which they consider as a northward extension of the Pollino fault (POL in Fig. 2).

## SEISMIC DATA ANALYSIS AND RESULTS

The ongoing phase of Pollino earthquake activity started during spring 2010 and has consisted of more than 4000 earthquakes of maximum local magnitude 5.0 that have occurred with a fairly regular increase of number and energy since the

onset of activity to date (Fig. 1b). A frequency-versus-magnitude plot of the earthquakes reported in the ISIDE database for the Pollino area between 1 April 2010 and 5 December 2012 is shown in Figure 1c.

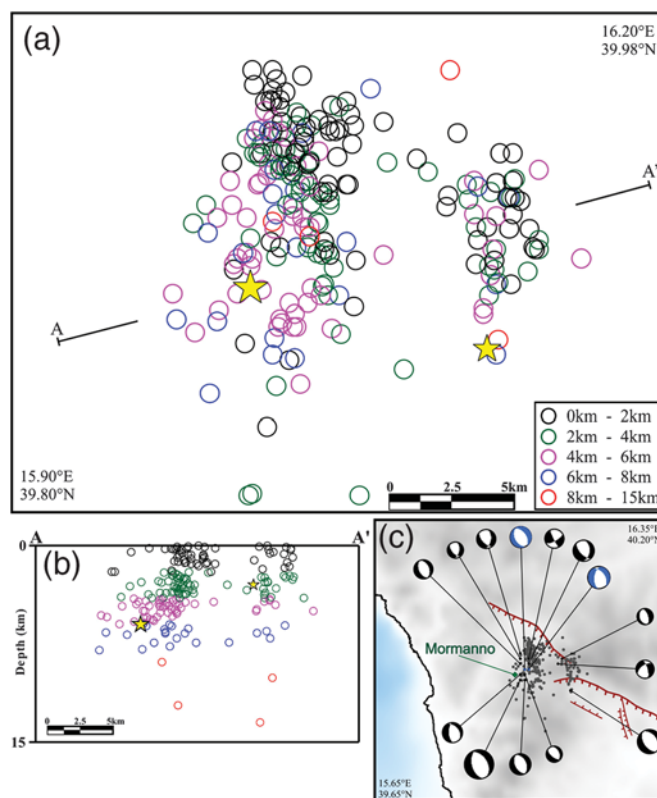
A map of the seismic stations used for the present analysis is given in Figure 3. We extracted from the INGV and University of Calabria databases the data of the earthquakes with local magnitude over 2.0 that occurred between 1 April 2010 and 5 December 2012 in the Pollino area (shaded zone in Fig. 3). We then calculated hypocenter locations using the Simulps algorithm by Evans *et al.* (1994) and the 3D velocity structure of the study region by Orecchio *et al.* (2011). We selected for graphical presentation of results in Figure 4a,b all the earthquakes located with at least eight *P* and nine *P* + *S* readings, and rms < 0.7 s. For these events we estimated, following the procedures by Presti *et al.* (2008), horizontal and vertical average location errors of the order of 1.5 and 1.7 km, respectively. Next, we performed an analysis of focal mechanisms by applying the Cut-and-Paste (CAP) waveform inversion method by Zhu and Helmberger (1996) and selected the best-constrained solutions (i.e., those solutions with fault parameter errors less than 10°; see also D'Amico *et al.*, 2010, 2011) that are shown in Figure 4c. Two spatial earthquake clusters can be detected in Figure 4a,b suggesting the presence of west-dipping north-northwest-trending sources. A *circa* 45° W-plunging elongated hypocenter cloud can be detected in Figure 4b for the western cluster. An apparently similar trend with higher dip, however, may be inferred from the same figure for the eastern cluster, although the smaller number of earthquakes and their discontinuous spatial distribution make the



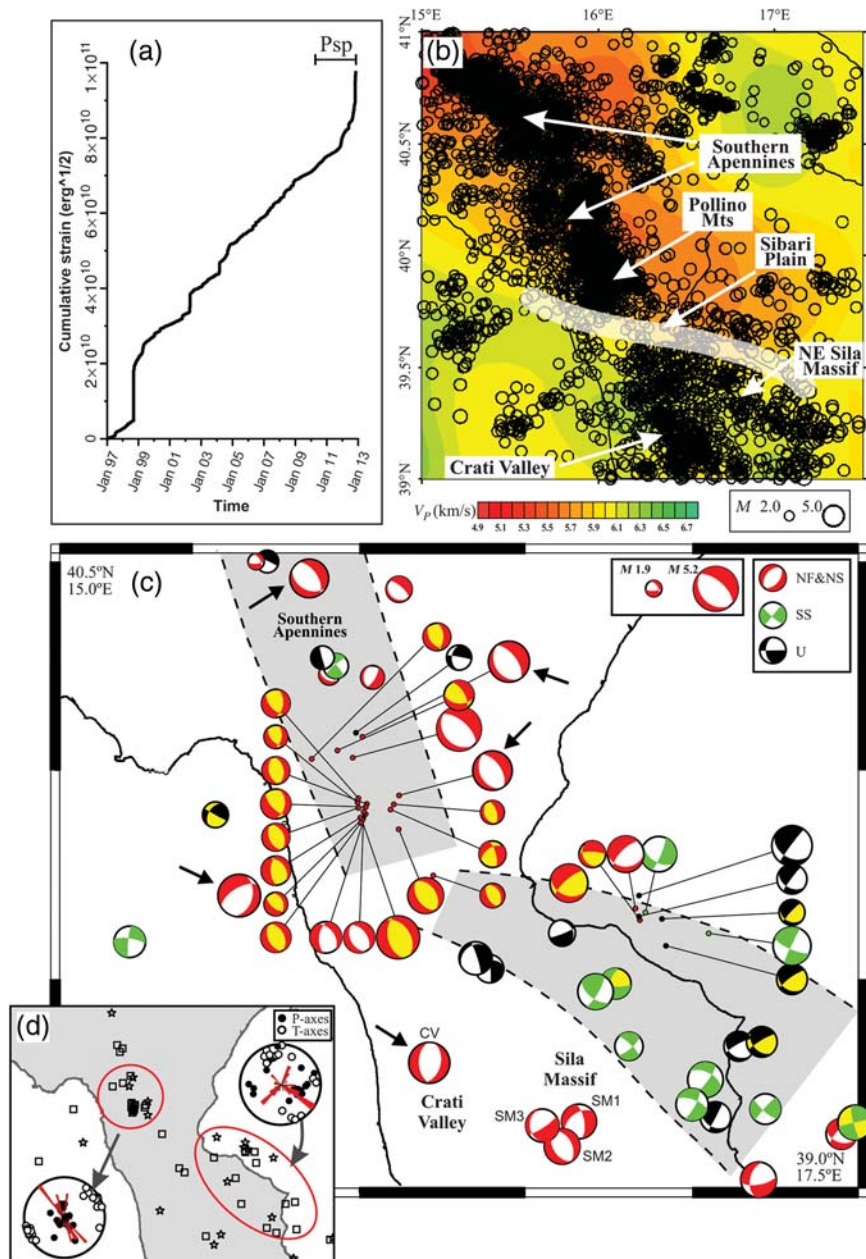
▲ **Figure 3.** Map of the seismic stations used in the present study with an enlarged view of the main study area. Empty triangles indicate stations installed after the onset of the ongoing Pollino crisis; full triangles, permanent stations operating in the region. The shadowed area corresponds to the seismic crisis area (see also earthquake locations in Fig. 4).

trend more doubtful in this case. The apparent north-northwest orientation of the two clusters matches well with the orientations of nodal planes from the focal mechanisms (Fig. 4c), which also indicate normal faulting.

An analysis of the crustal seismicity, which occurred in the wider area of northern Calabria and southern Apennines was then performed and the results are presented in Figure 5. In this case, a larger investigation time window (1 January 1997 to 5 December 2012) has been adopted. Figure 5a shows the cumulative seismic strain released over this wider area and



▲ **Figure 4.** Summary of the results obtained from the analysis of the Pollino earthquake activity, which occurred between 1 April 2010 and 5 December 2012. The sequence was still ongoing at the time of writing of this paper, in December 2012. (a) Epicenter map of the earthquakes located with a minimum of eight *P* and nine *P* + *S* readings and arrival-time rms < 0.7 s in the local velocity structure by Orecchio *et al.* (2011). Different colors indicate different hypocenter depths. Yellow stars show the locations of the two strongest earthquakes of magnitude 5.0 and 4.3 of 25 October and 28 May 2012, respectively. (b) Hypocenter vertical section of the earthquakes reported in plot (a). (c) Map of waveform-inversion focal mechanisms. Epicenter locations taken from (a) and the fault traces taken from Michetti *et al.* (2000) are also shown. Black and blue beach balls indicate the solutions estimated through the Cut-and-Paste (CAP) method in the present paper and those ones taken from the TDMT database (<http://cnt.rm.ingv.it/tdmt.html>, last accessed September 2013), respectively. The beach-ball size is proportional to the earthquake magnitudes that range between 2.7 and 5.0.



▲ **Figure 5.** Results from the analysis of the crustal seismicity (depth less than 30 km) occurred in the wider area of northern Calabria and southern Apennines between 1 January 1997 and 5 December 2012. Hypocenters were relocated in the 3D tomographic velocity model obtained by [Orecchio \*et al.\* \(2011\)](#). (a) Cumulative seismic strain release over the whole area and time window with indication of the Pollino sequence period (Psp). (b) Earthquake epicenter map plotted over the  $V_p$  tomographic plate at 10 km depth (tomography by [Orecchio \*et al.\*, 2011](#)). The white curve marks the transition between the low- $V_p$  domain of the southern Apennines and the high- $V_p$  domain of the Calabrian Arc. (c) Map of the waveform inversion focal mechanisms estimated in the present study (yellow background) or taken from the literature (TDMT database; [Presti \*et al.\*, 2013](#)). In addition to the focal mechanisms available for the 1 January 1997–5 December 2012 time window, the map also includes five good-quality solutions (indicated by arrows) available for the previous period, i.e., since 1980. Different colors in the legend mark different types of mechanisms according to the standard definitions of normal faulting (NF), normal faulting with minor strike-slip component (NS), strike-slip (SS), or unknown stress regime (U; [Zoback, 1992](#)). The beach-ball size is proportional to the earthquake magnitudes that range between 1.9 and 5.2. The two gray belts mark the two main faulting domains, i.e., the normal-faulting domain of the southern Apennines including the Pollino Mountains, and the left-lateral transtensional domain of northeastern Sila and Ionian coast. CV is the focal mechanism available for the Crati valley, whereas SM1, SM2, and SM3 are those available for the Sila Massif area. (d) Polar plots of the P and T axes and strikes of nodal planes (red rose diagram) for the earthquakes of section (c) located in the two selected areas of Pollino and northeastern Sila–Ionian coast, respectively. Squares and stars indicate earthquakes of magnitude less than 4.0 and in the range 4.0–5.2, respectively.

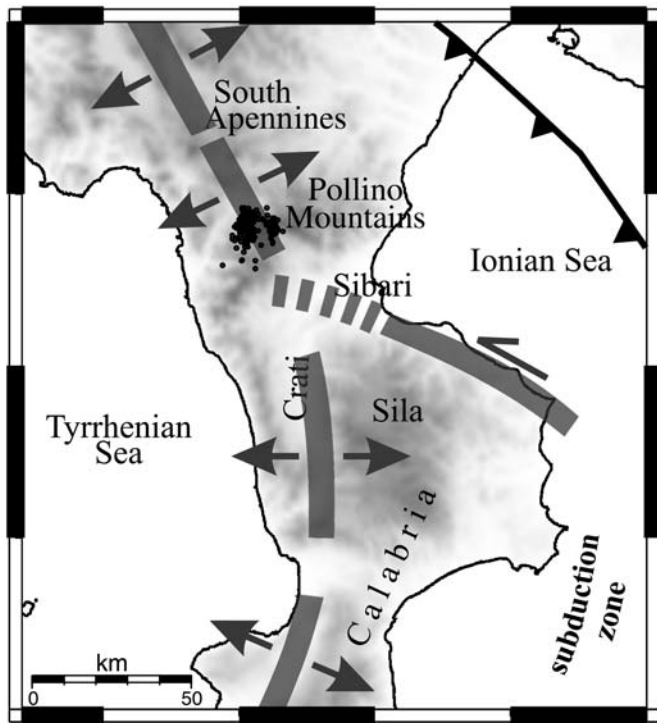
larger time window, and highlights the contribution by the Pollino sequence to seismic strain released in the last 15 years on a regional scale. Figure 5b displays the epicenters of the earthquakes of local magnitude over 2.0, occurred at depths shallower than 30 km during 1 January 1997–5 December 2012. These earthquakes have been relocated in the present work by using the 3D tomographic model by [Orecchio et al. \(2011\)](#). The epicenters are plotted over the tomographic results at 10 km depth. A south-southeast-trending epicenter cloud runs along the southern Apennines and covers also the Pollino area (Fig. 5b). This cloud is interrupted, toward south, at the latitude of the southern Pollino Mountains and Sibari Plain. In this area, with a white thick curve (Fig. 5b), we mark the transition between two different seismic-velocity domains evidenced by tomography: (1) the low- $V_p$  domain of the southern Apennines and (2) the high- $V_p$  one of the Calabrian Arc. To the south of the transitional white curve, the epicenter cloud reappears and shows separation in two branches. The major branch continues south-southeastward in the Crati valley and in the western Sila Massif, whereas the other one trends circa east-southeast and follows the eastern Sibari Plain, the northeastern Sila Massif and the nearby Ionian coast of Calabria (Fig. 5b). A shift can also be noted in Figure 5b between the southern Apennines epicenter cloud with its southern edge in the Pollino Mountains and the cloud reappearing south of the discussed transition zone. Figure 5c reports the best-quality focal mechanisms available in the same area of Figure 5b for the 1 January 1997–5 December 2012 time interval, with the addition of five good-quality solutions available for the previous period (these latter solutions are indicated by arrows). Figure 5b,c include the earthquakes of the 2010–2012 Pollino sequence reported in Figure 4a,c, and confirm that the Pollino earthquakes occurred along north-northwest-striking normal-fault surfaces in response to a perpendicular extension (Fig. 5d). To the south, the only focal mechanism available for the Crati valley (CV solution in Fig. 5c) indicates a similar regime but slightly rotated, with north-striking normal-fault surfaces responding to an east–west-oriented extension. Further extensional focal mechanisms are located in the middle of the Sila Massif (SM1, SM2, and SM3 in Fig. 5c). Toward the east, the seismotectonic regime of the northeast Sila and Ionian coastal area is rather different and more complex, principally with N120°-striking fault surfaces affected by left-lateral, strike- and oblique-slip movements (Fig. 5c,d). According to these data, the two branches of the epicenter cloud detected south of the transition zone (white thick curve in Fig. 5b) correspond to significantly different seismotectonic regimes, i.e., normal faulting in the south-southeast-trending branch of the Crati valley and western Sila area, and left-lateral transtensional faulting in the east-southeast-trending branch of the northeast Sila–Calabrian Ionian coast (Fig. 5c,d).

## DISCUSSION

Hypocenter locations and focal mechanisms of the 2010 to date Pollino seismicity (Fig. 4) suggest that this activity can

be ascribed to normal faulting on north-northwest-trending west-southwest-dipping dislocation surfaces consistent with the general seismotectonic frame of the southern Apennines (Fig. 1a; e.g., [Frepoli et al., 2011](#)). Also, the analysis of crustal seismicity in the wider area of northern Calabria and the southern Apennines over a larger time interval of circa 15 years (Fig. 5) shows a well-defined south-southeast-trending belt of normal-faulting earthquakes running along the southern Apennines and interrupted to the south at the latitude of the southern Pollino Mountains and Sibari plain. A rather different seismotectonic regime is detected just south, in the area of northeastern Sila and the nearby Ionian coast of Calabria (Fig. 5). Here, N120°-striking fault surfaces affected by left-lateral, strike- and oblique-slip movements are evidenced by our focal mechanisms (Fig. 5c,d) and by geologic data available from the literature (Fig. 2). This change corresponds to the horizontal variation of the seismic velocity structure shown in Figure 5b. All these data lead us to locate the transitional area between the domains of the southern Apennines (north) and the Calabrian Arc (south) roughly at the latitude of the white thick curve shown in Figure 5b. It should be remarked that south of the Pollino Mountains, the geodynamic setting is very intricate and is complicated by the lateral edge of the Calabrian subduction zone ([Faccenna et al., 2011](#); [Neri et al., 2012](#)). Since at least Neogene time, the Calabrian accretionary wedge has drifted southeastwards onto the retreating Ionian slab (Fig. 1a; see, among others, [Faccenna et al., 2004](#)). Several studies have pointed out how the drifting mechanism has also been made possible by the presence of northwest-striking strike-slip faults across Calabria, some of these faults being active until recent times and also in the present (e.g., [Van Dijk et al., 2000](#); [Speranza et al., 2011](#); [Neri et al., 2012](#)). In some instances, these faults have presumably constituted the shallow expression of the dynamics occurring at the lateral edge of the Ionian slab (e.g., [Govers and Wortel, 2005](#)). One of these strike-slip fault systems probably occurs south of the Pollino Mountains (Figs. 1a and 2) and appears to be seismically active at least in its eastern Ionian section including the Sibari plain, northeastern Sila, and the nearby Ionian coast (Fig. 5). This strike-slip domain, which is complicated by the rapid uplift of the Sila Massif and surrounding areas ([Faccenna et al., 2011](#)), separates the southern Apennines from most of Calabria, where the extensional tectonics is probably driven by backarc mechanisms. The data presented in Figures 4 and 5 give new support to this geodynamic scheme, improve its accuracy in correspondence with the northern edge of the Calabrian subduction zone, and allow us to interpret the 2010 to date Pollino activity as seismic deformation occurring inside the southern Apennines seismotectonic domain, specifically at its southern tip (Fig. 6).

Deeper investigation of the space–time evolution of the Pollino activity is going to be undertaken by this same team, profiting of new data that are starting to come from *in situ* recording stations managed by different institutions. This will allow for the production of a larger location and mechanism database of the ongoing sequence and, consequently, to better



▲ **Figure 6.** Sketch view of the main deformation processes detected by the analysis of crustal seismicity in the Pollino Mountains (see Fig. 4) and in a wider area including the southern Apennines and Calabria (Fig. 5). The ongoing phase of earthquake activity in the Pollino Mountains is interpreted as seismic deformation occurring inside the southern Apennines extensional domain, specifically at its southern tip. South of Pollino, a left-lateral transtensional east-southeast-trending fault zone (closely corresponding to interruption of the seismic belt and transition between low- and high- $V_p$  crustal domains; white curve in Fig. 5b) probably represents a shallow response to deeper dynamics occurring at the northern edge of the Calabrian subduction zone. The south-eastward-retreating Ionian subducting slab and backarc mechanisms and/or the collapse induced by the general uplift of Calabria would be the engine of the seismogenic extensional processes in western Calabria.

characterize the sequence itself. With this additional effort, we should also be able to better investigate the increasing rate and strain-release patterns observed since the beginning of the sequence. This feature, at a very early inspection, looks similar to some documented examples of microfracture temporal patterns preceding failures of rock samples subjected to progressive stress loading in laboratory experiments (see e.g., Meredith *et al.*, 1990; Sammonds *et al.*, 1992; Ponomarev *et al.*, 1997; Zang *et al.*, 1998; Lei *et al.*, 2004; Benson *et al.*, 2010). Also, comparisons with real patterns observed in other regions are being attempted. As regard to possible forthcoming major failures in the Pollino area, it should be considered that the limited and partly contrasting information locally available on fault location and geometry (see e.g., Michetti *et al.*, 2000; DISS Working Group, 2010) does not allow us to assume the con-

tinuity or structural link of the activated dislocation surfaces with other structures. Therefore, any hypotheses of a major seismogenic fault close to rupture are not properly founded. It can, however, be noted that the sharp geodynamic change attested by detection of a west-northwest-striking strike-slip domain and tomographic structure variation at the southern edge of the Pollino Mountains may, plausibly, cause mechanical disconnection between the north-northwest-trending normal-faulting seismogenic structures located north and south of the discussed strike-slip domain, respectively (Figs. 5 and 6). Moreover, the occurred activation of local shallow structures trending north-northwest–south-southeast in the Pollino area does not necessarily imply that major stress is loading on a fault comprising the activated structures or parallel to them, for example, other nearby and diversely oriented ones could be involved in the forthcoming phases of activity (as also indicated by laboratory experiments; see e.g., Lockner *et al.*, 1991; Lei *et al.*, 2004). In any case, the information currently available should drive the scientific community and the responsible institutions to carry out greater monitoring and investigational efforts in the Pollino area both for scientific and social reasons. ☒

## ACKNOWLEDGMENTS

This work has been supported by the 2012–2013 S1 Project (RU6 Università della Calabria) funded by Istituto Nazionale di Geofisica e Vulcanologia and Dipartimento della Protezione Civile of Italy. We thank the *SRL* Editor Jonathan M. Lees and an anonymous reviewer for comments and suggestions that allowed us to significantly improve the manuscript.

## REFERENCES

- Amoruso, A., L. Crescentini, G. Neri, B. Orecchio, and R. Scarpa (2006). Spatial relation between the 1908 Messina Straits earthquake slip and recent earthquake distribution, *Geophys. Res. Lett.* **33**, L17309, doi: [10.1029/2006GL027227](https://doi.org/10.1029/2006GL027227).
- Arrigo, G., Z. Roumelioti, C. Benetatos, A. Kiratzi, A. Bottari, G. Neri, D. Termini, A. Gorini, and S. Marcucci (2006). A source study of the 9 September 1998 ( $M_w$  5.6) Castelluccio earthquake in southern Italy using teleseismic and strong motion data, *Nat. Hazards* **37**, 245–262.
- Benson, P. M., S. Vinciguerra, P. G. Meredith, and R. P. Young (2010). Spatio-temporal evolution of volcano seismicity: A laboratory study, *Earth Planet. Sci. Lett.* **297**, no. 1–2, 315–323, doi: [10.1016/j.epsl.2010.06.033](https://doi.org/10.1016/j.epsl.2010.06.033).
- Billi, A., G. Barberi, C. Faccenna, G. Neri, F. Pepe, and A. Sulli (2006). Tectonics and seismicity of the Tindari fault system, southern Italy: Crustal deformations at the transition between ongoing contractional and extensional domains located above the edge of a subducting slab, *Tectonics* **25**, TC2006, doi: [10.1029/2004TC001763](https://doi.org/10.1029/2004TC001763).
- Billi, A., C. Faccenna, O. Bellier, L. Minelli, G. Neri, C. Piromallo, D. Presti, D. Scrocca, and E. Serpelloni (2011). Recent tectonic reorganization of the Nubia–Eurasia convergent boundary heading for the closure of the western Mediterranean, *Bull. Soc. Geol. Fr.* **182**, no. 4, 279–303.
- Billi, A., D. Presti, C. Faccenna, G. Neri, and B. Orecchio (2007). Seismotectonics of the Nubia plate compressive margin in the south-Tyrrhenian region, Italy: Clues for subduction inception, *J. Geophys. Res.* **112**, B08302, doi: [10.1029/2006JB004837](https://doi.org/10.1029/2006JB004837).

- Billi, A., D. Presti, B. Orecchio, C. Faccenna, and G. Neri (2010). Incipient extension along the active convergent margin of Nubia in Sicily, Italy: Cefalù–Etna seismic zone, *Tectonics* **29**, TC4026, doi: [10.1029/2009TC002559](https://doi.org/10.1029/2009TC002559).
- Bonini, M., F. Sani, G. Moratti, and M. G. Benvenuti (2011). Quaternary evolution of the Lucania Apennine thrust front area (southern Italy), and its relations with the kinematics of the Adria Plate boundaries, *J. Geodyn.* **51**, 125–140, doi: [10.1016/j.jog.2010.01.010](https://doi.org/10.1016/j.jog.2010.01.010).
- Catalano, S., C. Monaco, L. Tortorici, W. Paltrinieri, and N. Steel (2004). Neogene–Quaternary tectonic evolution of the southern Apennines, *Tectonics* **23**, doi: [10.1029/2003TC001512](https://doi.org/10.1029/2003TC001512).
- Cinti, F. R., M. Moro, D. Pantosti, L. Cucci, and G. D’Addezio (2002). New constraints on the seismic history of the Castrovillari fault in the Pollino gap (Calabria, southern Italy), *J. Seismol.* **6**, 199–217.
- D’Amico, S., and L. Scarfi (2012). Rilievo macrosismico degli effetti prodotti dal terremoto del Pollino del 26 ottobre 2012 alle ore 01:05 locali, *Report of the QUick Earthquake Survey Team*, available at [www.ingv.it](http://www.ingv.it); last accessed September 2013 (in Italian).
- D’Amico, S., B. Orecchio, D. Presti, A. Gervasi, L. Zhu, I. Guerra, G. Neri, and R. B. Herrmann (2011). Testing the stability of moment tensor solutions for small earthquakes in the Calabro–Peloritani Arc region (southern Italy), *Bollettino di Geofisica Teorica e Applicata* **52**, no. 2, 283–298.
- D’Amico, S., B. Orecchio, D. Presti, L. Zhu, R. B. Herrmann, and G. Neri (2010). Broadband waveform inversion of moderate earthquakes in the Messina Straits, southern Italy, *Phys. Earth Planet. In.* **179**, 97–106.
- Database of Individual Seismogenic Sources (DISS) Working Group (2010). Version 3.1.1: A compilation of potential sources for earthquakes larger than  $M$  5.5 in Italy and surrounding areas, <http://diss.rm.ingv.it/diss/> (last accessed September 2013).
- Evans, J. R., D. Eberhart-Phillips, and C. H. Thurber (1994). User’s manual for simulp12 for imaging  $V_p$  and  $V_p/V_s$ : A derivative of the “Thurber” tomographic inversion simul3 for local earthquakes and explosions, *U.S. Geol. Surv. Open-File Rept.* **94-431**.
- Faccenna, C., P. Molin, B. Orecchio, V. Olivetti, O. Bellier, F. Funicello, L. Minelli, C. Piromallo, and A. Billi (2011). Topography of the Calabria subduction zone (southern Italy): Clues for the origin of Mt. Etna, *Tectonics* **30**, TC1003, doi: [10.1029/2010TC002694](https://doi.org/10.1029/2010TC002694).
- Faccenna, C., C. Piromallo, A. Crespo-Blanc, and L. Jolivet (2004). Lateral slab deformation and the origin of the western Mediterranean arcs, *Tectonics* **23**, TC1012, doi: [10.1029/2002TC001488](https://doi.org/10.1029/2002TC001488).
- Frepoli, A., C. Maggi, G. B. Cimini, A. Marchetti, and M. Chiappini (2011). Seismotectonics of southern Apennines from recent passive seismic experiments, *J. Geodyn.* **51**, 110–124.
- Galli, P., and V. Bosi (2003). Catastrophic 1638 earthquakes in Calabria (southern Italy): New insights from paleoseismological investigation, *J. Geophys. Res.* **108**, doi: [10.1029/2001JB001713](https://doi.org/10.1029/2001JB001713).
- Galli, P., F. Galadini, and D. Pantosti (2008). Twenty years of paleoseismology in Italy, *Earth Sci. Rev.* **88**, 89–117.
- Galli, P., D. Molin, R. Camassi, and V. Castelli (2001). Il terremoto del 9 Settembre 1998 nel quadro della sismicità storica del confine calabro-lucano: Possibili implicazioni sismotettoniche, *Ital. J. Quat. Sci.* **14**, no. 1, 31–40 (in Italian).
- Govers, R., and M. J. R. Wortel (2005). Lithosphere tearing at STEP faults: Response to edges of subduction zones, *Earth Planet. Sci. Lett.* **236**, 505–523.
- Guidoboni, E., G. Ferrari, D. Mariotti, A. Comastri, G. Tarabusi, and G. Valentini (2007). CFTI4Med, Catalogue of Strong Earthquakes in Italy (461 B.C.–1997) and Mediterranean Area (760 B.C.–1500), Istituto Nazionale di Geofisica e Vulcanologia–Storia Geofisica Ambiente (INGV–SGA), available at <http://storing.ingv.it/cfti4med/> (last accessed September 2013).
- Lei, X., K. Masuda, O. Nishizawa, L. Jouriaux, J. Q. Liu, W. T. Ma, T. Satoh, and K. Kusunose (2004). Detailed analysis of acoustic emission activity during catastrophic fracture of faults in rock, *J. Struct. Geol.* **26**, no. 2, 247–258, doi: [10.1016/S0191-8141\(03\)00095-6](https://doi.org/10.1016/S0191-8141(03)00095-6).
- Lockner, D. A., J. D. Byerlee, V. Kuksenko, A. Ponomarev, and A. Sidorin (1991). Quasi-static fault growth and shear fracture energy in granite, *Nature* **350**, 39–42.
- Meredith, P. G., I. G. Main, and C. Jones (1990). Temporal variations in seismicity during quasi-static and dynamic rock failure, *Tectonophysics* **175**, no. 1–3, 249–268, doi: [10.1016/0040-1951\(90\)90141-T](https://doi.org/10.1016/0040-1951(90)90141-T).
- Michetti, A. M., L. Ferrelì, E. Esposito, S. Porfido, A. M. Blumetti, E. Vittori, L. Serva, and G. P. Roberts (2000). Ground effects during the 9 September 1998,  $M_w = 5.6$  Lauria earthquake and the seismic potential of the “aseismic” Pollino region in southern Italy, *Seismol. Res. Lett.* **71**, 31–46.
- Monaco, C., and L. Tortorici (2000). Active faulting in the Calabrian arc and eastern Sicily, *J. Geodyn.* **29**, 407–424.
- Montone, P., M. T. Mariucci, and S. Pierdominici (2012). The Italian present-day stress map, *Geophys. J. Int.* **189**, 705–716.
- Neri, G., G. Barberi, G. Oliva, and B. Orecchio (2004). Tectonic stress and seismogenic faulting in the area of the 1908 Messina earthquake, south Italy, *Geophys. Res. Lett.* **31**, L10602, doi: [10.1029/2004GL019742](https://doi.org/10.1029/2004GL019742).
- Neri, G., G. Barberi, G. Oliva, and B. Orecchio (2005). Spatial variations of seismogenic stress orientations in Sicily, south Italy, *Phys. Earth Planet. In.* **148**, 175–191.
- Neri, G., A. M. Marotta, B. Orecchio, D. Presti, C. Totaro, R. Barzaghi, and A. Borghi (2012). How lithospheric subduction changes along the Calabrian Arc in southern Italy: Geophysical evidences, *Int. J. Earth Sci.* **101**, 1949–1969.
- Neri, G., G. Oliva, B. Orecchio, and D. Presti (2006). A possible seismic gap within a highly seismogenic belt crossing Calabria and eastern Sicily, Italy, *Bull. Seismol. Soc. Am.* **96**, no. 4A, 1321–1331, doi: [10.1785/0120050170](https://doi.org/10.1785/0120050170).
- Neri, G., B. Orecchio, C. Totaro, G. Falcone, and D. Presti (2009). Subduction beneath southern Italy close the ending: Results from seismic tomography, *Seismol. Res. Lett.* **80**, no. 1, 63–70, doi: [10.1785/gssrl.80.1.63](https://doi.org/10.1785/gssrl.80.1.63).
- Orecchio, B., D. Presti, C. Totaro, I. Guerra, and G. Neri (2011). Imaging the velocity structure of the Calabrian Arc region (south Italy) through the integration of different seismological data, *Bollettino di Geofisica Teorica ed Applicata* **52**, 625–638.
- Ponomarev, A. V., A. D. Zavyalov, V. B. Smirnov, and D. A. Lockner (1997). Physical modeling of the formation and evolution of seismically active fault zones, *Tectonophysics* **277**, no. 1–3, 57–81, doi: [10.1016/S0040-1951\(97\)00078-4](https://doi.org/10.1016/S0040-1951(97)00078-4).
- Presti, D., A. Billi, B. Orecchio, C. Totaro, C. Faccenna, and G. Neri (2013). Earthquake focal mechanisms, seismogenic stress, and seismotectonics of the Calabrian Arc, Italy, *Tectonophysics* **602**, 153–175, doi: [10.1016/j.tecto.2013.01.030](https://doi.org/10.1016/j.tecto.2013.01.030).
- Presti, D., B. Orecchio, G. Falcone, and G. Neri (2008). Linear versus nonlinear earthquake location and seismogenic fault detection in the southern Tyrrhenian Sea, Italy, *Geophys. J. Int.* **172**, no. 2, 607–618, doi: [10.1111/j.1365-246X.2007.03642.x](https://doi.org/10.1111/j.1365-246X.2007.03642.x).
- Rovida, A., R. Camassi, P. Gasperini, and M. Stucchi (2011). CPTI11, la versione 2011 del Catalogo Parametrico dei Terremoti Italiani, Milano, Bologna, <http://emidius.mi.ingv.it/CPTI11>; last accessed September 2013 (in Italian).
- Sammonds, P. R., P. G. Meredith, and I. G. Main (1992). Role of pore fluids in the generation of seismic precursors to shear fracture, *Nature* **359**, 228–230, doi: [10.1038/359228a0](https://doi.org/10.1038/359228a0).
- Speranza, F., P. Macrì, D. Rio, E. Fornaciari, and C. Consolaro (2011). Paleomagnetic evidence for a post-1.2 Ma disruption of the Calabria terrane: Consequences of slab breakoff on orogenic wedge tectonics, *Bull. Geol. Soc. Am.* **123**, 925–933.
- Spina, V., E. Tondi, and S. Mazzoli (2011). Complex basin development in a wrench-dominated back-arc area: Tectonic evolution of the Crati basin, Calabria, Italy, *J. Geodyn.* **51**, 90–109.

- Van Dijk, J. P., M. Bello, G. P. Brancaleoni, G. Cantarella, V. Costa, A. Frixia, F. Golfetto, S. Merlini, M. Riva, S. Torricelli, C. Toscano, and A. Zerilli (2000). A regional structural model for the northern sector of the Calabrian Arc (southern Italy), *Tectonophysics* **324**, 267–320.
- Zang, A. R., F. C. Wagner, S. Stanchits, G. Dresen, R. Andresen, and M. A. Haidekker (1998). Source analysis of acoustic emissions in Aue granite cores under symmetric and asymmetric compressive loads, *Geophys. J. Int.* **135**, no. 3, 1113–1130, doi: [10.1046/j.1365-246X.1998.00706.x](https://doi.org/10.1046/j.1365-246X.1998.00706.x).
- Zhu, L., and D. Helmberger (1996). Advancement in source estimation technique using broadband regional seismograms, *Bull. Seismol. Soc. Am.* **86**, 1634–1641.
- Zoback, M. L. (1992). First- and second-order patterns of stress in the lithosphere: The World Stress Map project, *J. Geophys. Res.* **97**, 703–711.

*Cristina Totaro  
Debora Presti  
Barbara Orecchio  
Giancarlo Neri  
Dipartimento di Fisica e di Scienze della Terra  
Università di Messina  
V.le F. Stagno D'Alcontres, 31  
98166 Messina, Italy  
ctotaro@unime.it*

*Andrea Billi  
Consiglio Nazionale delle Ricerche  
Istituto di Geologia Ambientale e Geoingegneria (IGAG)  
Via Salaria Km 29,300  
Monterotondo, Rome, Italy*

*Anna Gervasi<sup>1</sup>  
Istituto Nazionale di Geofisica e Vulcanologia (INGV)  
Centro Nazionale Terremoti  
via Vigna Murata 605  
00143 Rome, Italy*

*Ignazio Guerra  
Dipartimento di Fisica  
Università della Calabria  
via Pietro Bucci  
87036 Arcavacata di Rende  
Cosenza, Italy*

---

<sup>1</sup> Also at Dipartimento di Fisica, Università della Calabria, Arcavacata di Rende, Cosenza, Italy.